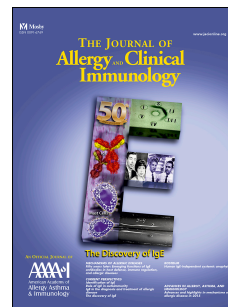


Accepted Manuscript

A Type III Complement Factor D Deficiency: Structural insights for inhibition of the alternative pathway

Christopher C.T. Sng, MB BChir, Sorcha O'Byrne, BSc, Daniil M. Prigozhin, PhD, Matthias R. Bauer, PhD, Jennifer C. Harvey, BSc, Michelle Ruhle, BBiomedSc, Ben G. Challis, PhD, Sara Lear, MBBS, Lee D. Roberts, PhD, Sarita Workman, RN MSc, Tobias Janowitz, PhD, Lukasz Magiera, PhD, Rainer Doffinger, PhD FRCPPath, Matthew S. Buckland, PhD FRCPPath, Duncan J. Jodrell, DM MSc FRCP, Robert K. Semple, MB PhD, Timothy J. Wilson, PhD, Yorgo Modis, PhD, James E.D. Thaventhiran, PhD FRCPPath



PII: S0091-6749(18)30327-0

DOI: [10.1016/j.jaci.2018.01.048](https://doi.org/10.1016/j.jaci.2018.01.048)

Reference: YMAI 13343

To appear in: *Journal of Allergy and Clinical Immunology*

Received Date: 24 October 2017

Revised Date: 2 January 2018

Accepted Date: 16 January 2018

Please cite this article as: Sng CCT, O'Byrne S, Prigozhin DM, Bauer MR, Harvey JC, Ruhle M, Challis BG, Lear S, Roberts LD, Workman S, Janowitz T, Magiera L, Doffinger R, Buckland MS, Jodrell DJ, Semple RK, Wilson TJ, Modis Y, Thaventhiran JED, A Type III Complement Factor D Deficiency: Structural insights for inhibition of the alternative pathway, *Journal of Allergy and Clinical Immunology* (2018), doi: 10.1016/j.jaci.2018.01.048.

This is a PDF file of an unedited manuscript that has been accepted for publication. As a service to our customers we are providing this early version of the manuscript. The manuscript will undergo copyediting, typesetting, and review of the resulting proof before it is published in its final form. Please note that during the production process errors may be discovered which could affect the content, and all legal disclaimers that apply to the journal pertain.

1 **TITLE PAGE**

2

3 Letter to the Editor

4

5 **A Type III Complement Factor D Deficiency: Structural insights for inhibition of the**
6 **alternative pathway.**

7

8 Christopher C. T. Sng, MB BChir,^{1*} Sorcha O'Byrne, BSc,^{2*} Daniil M. Prigozhin, PhD^{3*},9 Matthias R. Bauer, PhD,^{4*} Jennifer C. Harvey, BSc,⁵ Michelle Ruhle, BBiomedSc,⁶ Ben G.10 Challis, PhD,⁷ Sara Lear, MBBS,² Lee D. Roberts, PhD,⁹ Sarita Workman, RN MSc,⁵ Tobias11 Janowitz, PhD,¹ Lukasz Magiera, PhD,¹ Rainer Doffinger, PhD FRCPATH,² Matthew S.12 Buckland, PhD FRCPATH,⁵ Duncan J. Jodrell, DM MSc FRCP,¹ Robert K. Semple, MB PhD,⁷13 ⁸ Timothy J. Wilson, PhD,¹⁰ Yorgo Modis, PhD,³ James E. D. Thaventhiran, PhD FRCPATH.¹14 ^{2 11 12}

15

16 ¹Cancer Research UK Cambridge Institute, Robinson Way, Cambridge, CB2 0RE U.K.17 ²Department of Clinical Immunology, Cambridge University Hospitals NHS Trust,

18 Addenbrooke's Hospital, Cambridge, CB2 0QQ U.K.

19 ³Molecular Immunity Unit, Department of Medicine, MRC Laboratory of Molecular Biology,

20 Cambridge Biomedical Campus, Francis Crick Ave, Cambridge CB2 0QH, U.K.

21 ⁴MRC Laboratory of Molecular Biology, Cambridge Biomedical Campus, Francis Crick

22 Ave, Cambridge CB2 0QH, U.K.

23 ⁵Department of Immunology, Royal Free London NHS Foundation Trust, Pond Street,

24 Hampstead, London, NW3 2QG U.K.

- 25 ⁶The Walter and Eliza Hall Institute of Medical Research, 1G Royal Parade, Parkville,
26 Victoria, Australia 3058
- 27 ⁷Wellcome Trust-MRC Institute of Metabolic Science, Addenbrooke's Hospital, Cambridge,
28 CB2 0QQ U.K.
- 29 ⁸University of Edinburgh Centre for Cardiovascular Sciences, Queen's Medical Research
30 Institute, Little France Crescent, Edinburgh EH16 4TJ.
- 31 ⁹Leeds Institute of Cardiovascular and Metabolic Medicine, LIGHT Laboratories
32 University of Leeds, LS2 9JT U.K.
- 33 ¹⁰Department of Microbiology, Miami University, 68 Pearson Hall, 700 E. High Street,
34 Oxford, OH 45056 U.S.A.
- 35 ¹¹Department of Medicine, University of Cambridge, Addenbrooke's Hospital, Cambridge,
36 CB2 0QQ U.K.
- 37 ¹²MRC Toxicology Unit, Hodgkin Building, University of Leicester, LE1 9HN U.K.
- 38 * These authors contributed equally to this work.
- 39
- 40 Corresponding author
- 41 James E. D. Thaventhiran, PhD
- 42 Department of Medicine
- 43 Addenbrooke's Hospital
- 44 Box 157
- 45 Hills Rd
- 46 Cambridge
- 47 CB2 0QQ U.K.
- 48
- 49 Telephone: +44 7740 703599

50 Fax: +44 1223 336846

51 E-mail: jedt2@cam.ac.uk

52

53 Declaration of all sources of funding: JEDT is supported by an MRC Clinician Scientist

54 Fellowship (MR/L006197/1). This work was funded by BRC III PPG funding and a

55 Wellcome Trust Senior Research Fellowship to Y.M. (101908/Z/13/Z). RKS is funded by the

56 Wellcome Trust [grant number WT098498 and strategic award 100574/Z/12/Z], the United

57 Kingdom Medical Research Council [MRC_MC_UU_12012/5] and the United Kingdom

58 National Institute for Health Research (NIHR) Cambridge Biomedical Research Centre. TJ is

59 funded by Cancer Research UK (Clinician Scientist Fellowship C42738/A24868). BGC is

60 now a full-time employee of Astra-Zeneca.

61

62 Word count: 1012

63

64 Capsule summary

65 We fully characterise the first reported functional deficiency of complement factor D in a
66 patient. The structural analysis yielded a novel approach by which this key enzyme could be
67 inhibited to treat inflammatory diseases.

68 Key words

69 Adipsin, age-related macular degeneration, alternative pathway, complement deficiency,
70 complement serine protease, drug development, factor D, glucose homeostasis, single-
71 nucleotide variant, type III deficiency

72

73 Abbreviations used

74 AMD: age-related macular degeneration

75 AP: alternative complement pathway

76 AP50: alternative pathway haemolytic activity

77 CH50: classical pathway haemolytic activity

78 FB: complement factor B

79 FD: complement factor D

80 MD: molecular dynamics

81 WT: wild-type

82 To the Editor:

83 We investigated an alternative complement pathway (AP) deficiency in a patient with absent
84 alternative pathway haemolytic activity (AP50) but normal classical pathway haemolytic
85 activity recovering from invasive meningococcal infection (for patient and sibling details, see
86 Appendix A in this article's Online Repository). Serum reconstitution with proximal AP
87 components suggested a Factor D (FD) deficiency (Fig 1A). Sanger sequencing of *CFD*
88 identified a rare homozygous missense mutation (c.602G>C) in exon 4 in the patient (II-1)
89 and sibling (II-2), resulting in an arginine to proline substitution (p. R176P) (see Fig E1, A, in
90 this article's Online Repository). This genotype co-segregated with an AP50-null phenotype,
91 as the parents, both heterozygotes, had normal AP50 (Fig 1B). In contrast to previous
92 confirmed FD deficiencies,¹⁻³ all members of the pedigree had normal levels of circulating
93 FD, as corroborated by western blot (see Fig E1, B). Meanwhile, identical circular dichroism
94 spectra and melting curves of recombinant wild-type (WT) and R176P FD precluded gross
95 changes in FD structure or stability, suggesting a functional deficiency (Fig 1C and see Fig
96 E1, C). We assessed the cleavage of C3b-bound Factor B (FB) by recombinant WT and
97 mutant FD (R176P, R176A, R176Q). WT FD could cleave C3b-bound FB to produce
98 fragments Bb and Ba. Conversely, R176P FD demonstrated diminished *in vitro* catalytic
99 activity at all concentrations, and had negligible activity at physiological concentration (0.04
100 μ M) (Fig 1D and see E1, D). Reconstitution of FD-depleted serum with R176P FD also
101 demonstrated impaired AP mediated haemolysis (see Fig E1, E).

102

103 FD's serine protease activity depends on obligatory binding to the C3bB complex via four
104 exosite loops (residues 132-135, 155-159, 173-176, 203-209). This leads to rearrangement of
105 the self-inhibitory loop (199-202), allowing realignment of His41 and Asp89 with Ser183 to
106 form the active catalytic triad (see Fig E2, A and B, in this article's Online Repository).^{4,5}

107 Mutation R176P lies outside the active site, within one of the FB-binding exosite loops. We
108 used molecular dynamics (MD) stimulations to study how the R176P mutation affects the FD
109 protein fold (see Fig E2, C). In mutant FD, we observed a rearrangement of the exosite loop
110 155-161 within 50 ns of simulation (Fig 2A). This was unexpected because loop 155-161 was
111 not in direct contact with residue 176. Average structures generated from the final 50 ns of
112 simulation for WT and mutant FD (R176P and R176A) demonstrated that key FB-binding
113 residues Asp161 and Arg157 were shifted by 4.3 Å and 1.9 Å respectively (C α average
114 position) (Fig 2B). Superimposing these MD average structures onto the crystal structure of
115 the C3bB-D complex revealed that Asp161 and Arg157 assumed a conformation that no
116 longer supported binding due to loss of shape and charge complementarity to the FB surface
117 (Fig 2C). The other three exosite loops retained their binding-competent conformations. After
118 assuming the new conformation, exosite loop 155-161 demonstrated higher conformational
119 mobility (root mean square fluctuation) relative to WT (Fig E2, D and E). In contrast, the
120 mobility of loops containing catalytic residues His41 and Asp89 decreased in the mutants.
121 Using the distance between His41 and Ser183 during MD simulations as a proxy for the
122 active site conformation, we observed that WT could sample the short distance necessary for
123 a catalytically active conformation (Fig 2D). Conversely, in both mutant simulations, the
124 distance remained larger, consistent with His41 pointing away from the active site. Therefore,
125 in addition to disruption of key FB-binding residues, mutations R176P and R176A appear to
126 stabilise the self-inhibited conformation of free FD.

127

128 To assess the binding of FD to C3bB, we used surface plasmon resonance. Co-injection of
129 catalytically inactive FD (WT/S183A) with FB demonstrated a dose-dependent increase in
130 binding to C3b and complex formation (Fig 2E). In contrast, R176P/S183A FD lacked any
131 detectable binding (Fig 2F). Consistent with the stochastic transitions of free WT FD to the

132 active conformation observed in the MD simulation, FD has a low level of esterolytic activity
133 towards a small synthetic substrate, Z-Lys-SBzl (Fig 2D). Surprisingly, R176P FD
134 demonstrated a loss of esterolytic activity similar to the active site mutant, S183A (see Fig
135 2G).

136

137 Deficiency of properdin, the most common AP deficiency, can result from absent (type I),
138 low (type II) or normal but non-functioning (type III) protein levels (for reference, see
139 Reference E10 in this article's Online Repository). Meanwhile, previously confirmed
140 deficiencies of activating complement serine proteases have all resulted in low or absent gene
141 product. We have identified a unique deficiency: R176P FD is fully expressed and stable, but
142 enzymatically inert, constituting a functional or Type III deficiency. Recent preclinical
143 evidence⁶ that FD deficient mice are susceptible to diabetes prompted metabolic assessment
144 in the FD deficient patients. No abnormality was detected (for details, see Appendix B, Fig
145 E3 and Table E1 in this article's Online Repository).

146

147 Over-activation of AP is implicated in numerous inflammatory disorders, including age-
148 related macular degeneration (AMD). Therefore, blockade of the AP by targeting the rate-
149 limiting enzyme, FD, is an attractive approach to controlling disease progression. An anti-FD
150 Fab fragment targeting the two distal exosite loops has shown some benefit in phase II
151 clinical trials for treatment of dry AMD.⁷ *In vitro* studies indicate that it inhibits binding to
152 the C3bB complex but *increases* esterolytic activity towards small-molecule substrates.⁸ This
153 may result in unwanted clinical effects due to non-specific activity or limit its efficacy *in*
154 *vivo*. In the case of R176P FD, both FB-binding *and* esterolytic activity are abrogated
155 through exosite hindrance and stabilisation of the self-inhibited state. Loop 173-176 is thus a
156 promising target for allosteric inhibitors of FD that stabilise the inhibitory loop in addition to

157 binding-blockade. A structure-based design approach to targeting FD has recently succeeded
158 in identifying candidate FD inhibitors where high-throughput screens had failed,⁹
159 highlighting the benefits of integrating structural information into candidate drug screens.
160 Comprehensive definition of the structural and molecular determinants of *in vivo* FD activity
161 is critical for this. This study of the R176P mutation demonstrates how in-depth mechanistic
162 analysis of rare complement deficiencies can deliver such insight validated clinically by *in*
163 *vivo* human evidence of AP blockade.

164

165 Our acknowledgements can be found in this article's Online Repository.

166

167 Christopher C. T. Sng, MB BChir^{1*}

168 Sorcha O'Byrne, BSc^{2*}

169 Daniil M. Prigozhin, PhD^{3*}

170 Matthias R. Bauer, PhD^{4*}

171 Jennifer C. Harvey, BSc⁵

172 Michelle Ruhle, BBiomedSc⁶

173 Ben G. Challis, PhD⁷

174 Sara Lear, MBBS²

175 Lee D. Roberts, PhD⁹

176 Sarita Workman, RN MSc⁵

177 Tobias Janowitz, PhD¹

178 Lukasz Magiera, PhD¹

179 Rainer Doffinger, PhD FRCPATH²

180 Matthew S. Buckland, PhD FRCPATH⁵

181 Duncan J. Jodrell, DM MSc FRCP¹

182 Robert K. Semple, MB PhD^{7 8}

183 Timothy J. Wilson, PhD¹⁰

184 Yorgo Modis, PhD³

185 James E. D. Thaventhiran, PhD FRCPath^{1 2 11 12}

186

187 From ¹Cancer Research UK Cambridge Institute, Cambridge, United Kingdom; ²Department
188 of Clinical Immunology, Cambridge University Hospitals NHS Trust, Addenbrooke's
189 Hospital, Cambridge, United Kingdom; ³Molecular Immunity Unit, Department of Medicine,
190 MRC Laboratory of Molecular Biology, Cambridge, United Kingdom; ⁴MRC Laboratory of
191 Molecular Biology, Cambridge, United Kingdom; ⁵Department of Immunology, Royal Free
192 London NHS Foundation Trust, London, United Kingdom; ⁶The Walter and Eliza Hall
193 Institute of Medical Research, Parkville, Victoria, Australia; ⁷Wellcome Trust-MRC Institute
194 of Metabolic Science, Addenbrooke's Hospital, Cambridge, United Kingdom; ⁸University of
195 Edinburgh Centre for Cardiovascular Sciences, Queen's Medical Research Institute, Little
196 France Crescent, Edinburgh EH16 4TJ; ⁹Leeds Institute of Cardiovascular and Metabolic
197 Medicine, LIGHT Laboratories, University of Leeds, Leeds, United Kingdom; ¹⁰Department
198 of Microbiology, Miami University, Oxford, United States of America; ¹¹Department of
199 Medicine, University of Cambridge, Addenbrooke's Hospital, Cambridge, United Kingdom;
200 and the ¹²MRC Toxicology Unit, Hodgkin Building, University of Leicester, LE1 9HN
201 United Kingdom.

202 * These authors contributed equally to this work.

203

204

205 **References**

- 206 1. Hiemstra PS, Langelier E, Compier B, Keepers Y, Leijh PC, van den Barselaar MT, et
207 al. Complete and partial deficiencies of complement factor D in a Dutch family. *J*
208 *Clin Invest* 1989; 84:1957-61.
- 209 2. Biesma DH, Hannema AJ, van Velzen-Blad H, Mulder L, van Zwieten R, Kluijt I, et
210 al. A family with complement factor D deficiency. *J Clin Invest* 2001; 108:233-40.
- 211 3. Sprong T, Roos D, Weemaes C, Neeleman C, Geesing CL, Mollnes TE, et al.
212 Deficient alternative complement pathway activation due to factor D deficiency by 2
213 novel mutations in the complement factor D gene in a family with meningococcal
214 infections. *Blood* 2006; 107:4865-70.
- 215 4. Narayana SV, Carson M, el-Kabbani O, Kilpatrick JM, Moore D, Chen X, et al.
216 Structure of human factor D. A complement system protein at 2.0 Å resolution. *J Mol*
217 *Biol* 1994; 235:695-708.
- 218 5. Forneris F, Ricklin D, Wu J, Tzekou A, Wallace RS, Lambris JD, et al. Structures of
219 C3b in complex with factors B and D give insight into complement convertase
220 formation. *Science* 2010; 330:1816-20.
- 221 6. Lo JC, Ljubicic S, Leibiger B, Kern M, Leibiger IB, Moede T, et al. Adipsin is an
222 adipokine that improves beta cell function in diabetes. *Cell* 2014; 158:41-53.
- 223 7. Yaspan BL, Williams DF, Holz FG, Regillo CD, Li Z, Dressen A, et al. Targeting
224 factor D of the alternative complement pathway reduces geographic atrophy
225 progression secondary to age-related macular degeneration. *Sci Transl Med* 2017; 9.
- 226 8. Katschke KJ, Jr., Wu P, Ganesan R, Kelley RF, Mathieu MA, Hass PE, et al.
227 Inhibiting alternative pathway complement activation by targeting the factor D
228 exosite. *J Biol Chem* 2012; 287:12886-92.

- 229 9. Maibaum J, Liao SM, Vulpetti A, Ostermann N, Randl S, Rudisser S, et al. Small-
230 molecule factor D inhibitors targeting the alternative complement pathway. Nat Chem
231 Biol 2016; 12:1105-10.

232

233

ACCEPTED MANUSCRIPT

234 **Figure legends**235 **Figure 1:** Assessing the contribution of mutation R176P to AP dysfunction.236 (A) AP50 assay assessing patient serum supplemented with properdin (P), factor B (FB) or
237 factor D (FD).238 (B) The immediate family pedigree of the patient with the *CFD* genotype, serum AP50 and
239 serum FD concentrations displayed. *D*, WT allele. *d*, mutant allele (c.602G>C).

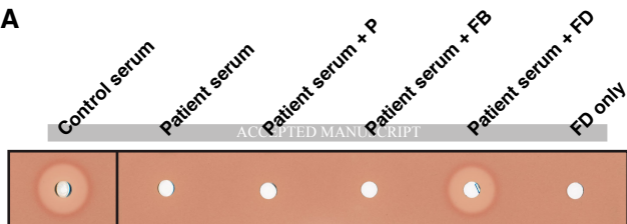
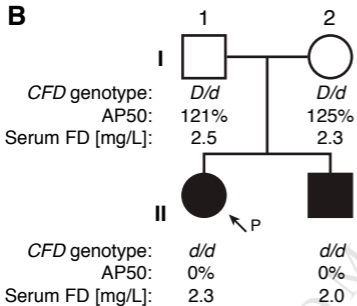
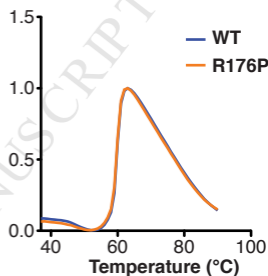
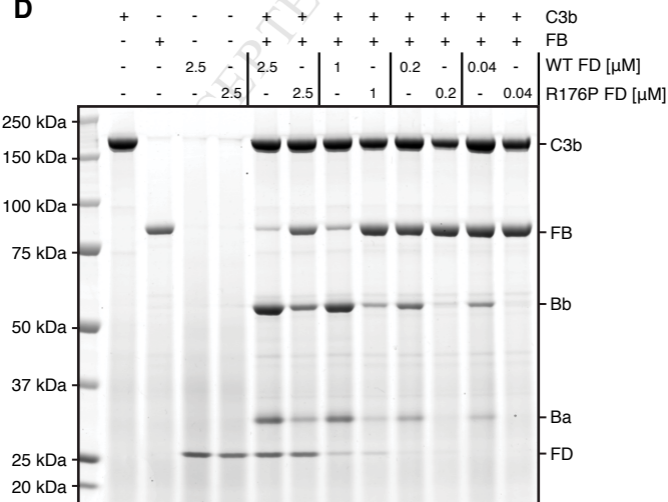
240 (C) Thermal shift assay of WT and R176P FD.

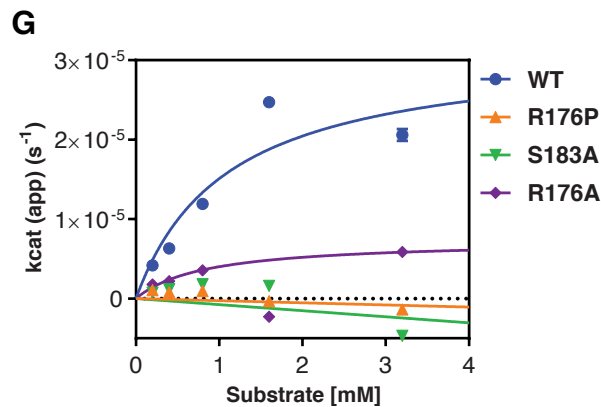
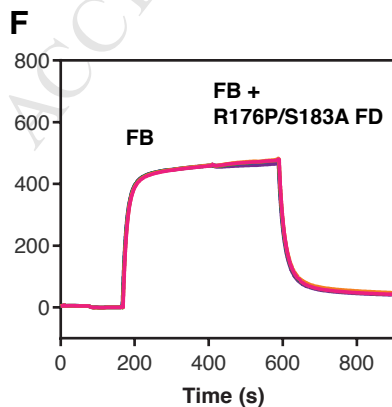
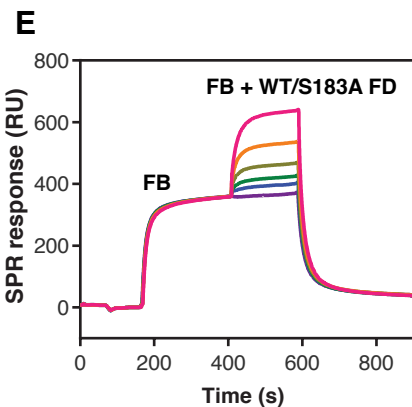
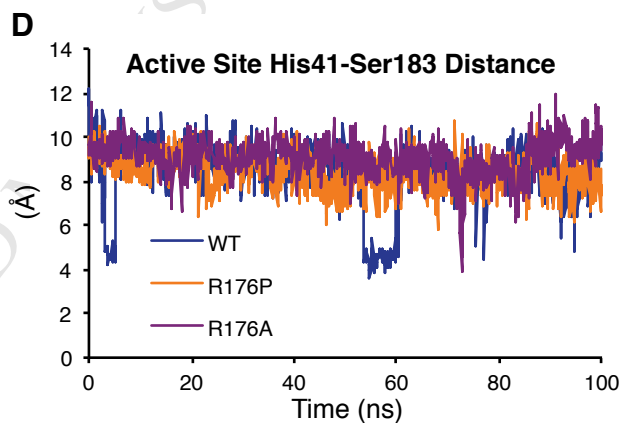
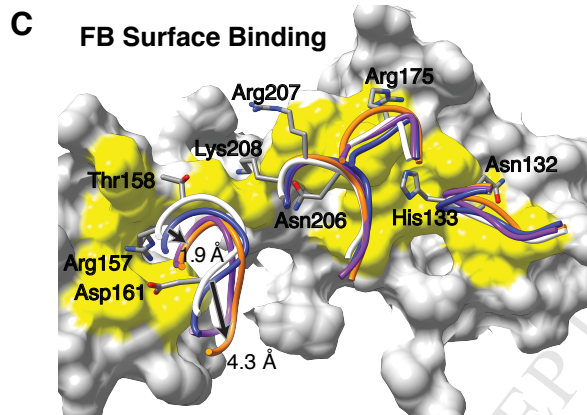
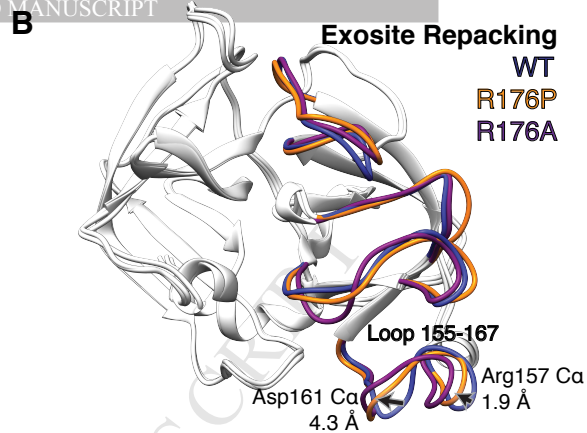
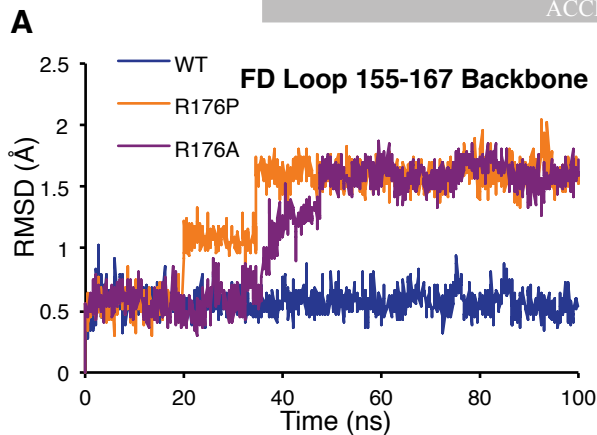
241 (D) Serial dilutions of recombinant WT or R176P FD were incubated with C3b and FB. The
242 SDS-PAGE gel, stained with AcquaStain, shows the individual proteins and resultant
243 products.244
245 **Figure 2:** Defining the effects of the R176P mutation on FD function.246 (A and B) FB-binding exosite loop 155-167 assumes a new conformation in mutant FD
247 simulation. Arrows highlight average C α position shifts of two residues that bind C3bB in the
248 R176P FD simulation.249 (C) Loss of shape complementarity at the FD-C3bB interface. FD exosite loops from
250 published co-crystal structures (white, PDB ID: 2XWB) overlaid with the simulated loops of
251 WT and mutant FD.252 (D) Distance sampled between the active site N ϵ 2 nitrogen of His41 and O γ of Ser183 during
253 each simulation. The shorter distance is necessary for catalytic activity.

254 (E and F) SPR binding measurement of enzymatically inactive recombinant FD

255 (R176P/S183A or WT/S183A) to C3bB complex.

256 (G) Steady state kinetics for Z-Lys-SBzl cleavage by WT, R176P, R176A and catalytically
257 inactive control S183A FD.

A**B****C****D**



1 APPENDIX A**2 Patient details**

3 A 19-year-old, South Asian female presented with a 24-hour history of high fever, rigors,
4 delirium and diarrhoea. On clinical examination, she was febrile with a purpuric rash and a
5 reduced level of consciousness (Glasgow Coma scale score: 9/15). Intravenous antibiotic
6 therapy was initiated for provisionally diagnosed meningococcal septicaemia. She was
7 intubated and transferred to the intensive care unit where she developed disseminated
8 intravascular coagulation, for which she received treatment. Results from blood cultures
9 drawn at the time of admission confirmed an infection with *Neisseria meningitidis* serogroup
10 Y. Her clinical condition improved with intensive care support and antimicrobial therapy.
11 She was discharged after two weeks with minimal sequelae including bilateral leg scarring, a
12 sacral pressure sore and mild bilateral hearing loss.

13
14 At the age of 5 years, she had received bilateral tympanostomy tubes for recurrent ear
15 infections and otitis media with effusion but had no other unusual infections as a child. She
16 received the full course of childhood vaccinations as per the national immunisation schedule.

17
18 On screening for immunodeficiency, laboratory measurement demonstrated a normal full
19 blood count with normal counts of lymphoid cells. The titres of C3, C4, mannose-binding
20 lectin and C1q were within normal range, but there was undetectable alternative
21 pathway haemolytic activity (AP50) in conjunction with normal classical pathway haemolytic
22 activity. In view of her complement deficiency, she was prescribed lifelong
23 phenoxymethylpenicillin as antimicrobial prophylaxis. She was also vaccinated for
24 meningitis ACWY, meningitis C, pneumococcus and haemophilus influenza B to which she
25 developed high antibody titre responses.

26

27 Her sole sibling, a younger male, who was homozygous for the same mutation, leading to an
28 identical pattern on immunodeficiency screening, was healthy at assessment. He reported no
29 excess of infections in the past. Of note, he reported having been treated empirically for
30 suspected meningitis, aged 11, whilst travelling in Mauritius from which he recovered with
31 no sequelae after a standard course of antibiotics.

32

33 **APPENDIX B**

34 **Functional Factor D deficiency does not result in impaired oral glucose tolerance**

35 Recent pre-clinical evidence^{E1} that FD regulates insulin secretion prompted metabolic
36 assessment of the patient and her sibling. They had a BMI of 19.3 kg/m² and 23.1 kg/m²,
37 respectively. Fasting venous plasma glucose (5.2-5.4 mmol/L) and insulin (29-39 pmol/L)
38 levels were normal in both subjects (Fig E3). Similarly, plasma glucose excursions were
39 normal in response to an oral glucose (75g) challenge. At 120 minutes following glucose
40 administration, glucose levels remained normal (4.0 mmol/L). Furthermore, circulating
41 concentrations of leptin and adiponectin, adipokines which regulate insulin sensitivity, were
42 normal, as were fasting lipid profiles in both subjects. Thus, glucose homeostasis is not
43 impaired in the context of genetic, and therefore lifelong, FD deficiency.

44

45 These results are consistent with the finding that FD knock-out mice developed impaired
46 glucose tolerance only on a long-term diabetogenic diet. This suggests that FD may
47 contribute little to glucose homeostasis in the absence of prolonged metabolic stress.

48 Alternatively, the role of FD in glucose homeostasis could be independent of binding to
49 C3bB or independent of its serine protease activity and, by extension, independent of its
50 downstream effects on the complement cascade. While congenital deficiency of FD alone

- 51 may not lead to insulin insufficiency, Lo et al.'s findings warrant observation of oral glucose
52 tolerance in such FD deficient patients under extreme metabolic stress and at older age.
53 Further research will be required to understand the role of FD in glucose homeostasis and
54 FD-deficient family pedigrees offer a useful clinical insight to this question.

ACCEPTED MANUSCRIPT

55 METHODS**56 Informed consent statement**

57 All study participants gave their informed consent as appropriate under approved protocols
58 from local institutional review boards. The research was conducted at University College
59 London and the University of Cambridge under approved protocols (#04/Q0501/119 for
60 affected individuals, #07/H0720/182 for family members).

61

62 Alternative pathway haemolytic activity measurement

63 AP100 RC003.1 Kit (Binding Site) agar-chicken erythrocyte plates were prepared according
64 to the manufacturer's instructions, with kit control and calibration solutions added. 5µl
65 aliquots of test serum were added to individual wells on the plates over ice. The loaded plates
66 were then stored at 4°C for 18 hours to allow radial diffusion of serum components, followed
67 by incubation at 37°C for 90 minutes to develop zones of lysis. The plates were then digitally
68 scanned at high-resolution, and the diameters of zones of lysis were measured using ImageJ
69 1.x computer software. Representative plates were selected for figures. The diameter of lysis
70 correlates with alternative pathway activity (AP50) and is expressed out of 100% relative to
71 kit control. Purified human Factor D (FD), Factor B and properdin for reconstitution assays
72 were purchased from Complement Tech, Inc.

73

74 Sanger sequencing

75 Genomic DNA was isolated from blood samples with QIAamp Kits (QIAGEN). The *CFD*
76 gene polymerase chain reaction was performed with primers annealing to intron sequences
77 close to each exon as described previously^{E2}. Specifically, regarding the R176P mutation, a
78 258-bp genomic fragment comprising exon 4 was amplified by PCR with the primers 5'-
79 CTGGGGCATAGTCAACCAC-3' and 5'-TGGGCCCTGTTCCCTACTTG-3'. The cDNA

80 numbering for the *CFD* variant identified is based on transcript NCBI Ref Seq accession no.
81 NM_001928/Ensembl accession no. ENST00000327726.6, beginning at the ATG start
82 codon. The genomic coordinates refer to the GRCh37 genome build.

83

84 **Western blot analysis**

85 Pooled control and the patient serum were diluted to 1:40 in tris-buffered saline and resolved
86 by SDS-PAGE on NuPAGE 4-12% Bis-Tris Gels, then blotted to nitrocellulose membranes.
87 FD was detected using goat anti-human FD (AF1824; R&D) and donkey anti-goat-IgG
88 IRDye 680CW (LI-COR Biosciences, Lincoln, NE, USA) secondary antibodies. The
89 membranes were imaged using the Odyssey Infrared Imaging System (LI-COR Biosciences,
90 Nebraska, USA)

91

92 **Recombinant CFD expression and purification**

93 Lentiviral transfer plasmid, envelope plasmid (pMD2.G; gift from Didier Trono; AddGene
94 plasmid #12260) and packaging plasmid (psPAX2; AddGene; gift from Didier Trono;
95 AddGene plasmid #12259) were used to transfect HEK293T cells to produce lentiviral
96 particles. The transfer vector (modified pLenti-CMV-GFP-Puro; gift of Eric Campeau –
97 Addgene 17448) included human FD cDNA (WT, R176P, R176A, S183A) with C-terminus
98 hexahistidine tag upstream of an IRES-Thy1.1 and a puromycin resistance gene (Puro^R).
99 Transfection was carried out using Lipofectamine 3000 and, after 24hrs, the media containing
100 the lentiviral particles was used immediately to stably transduce newly plated HEK293T
101 cells. After puromycin selection, stably transduced 293T cells were incubated with FreeStyle
102 media (Gibco) supplemented with 6X Glutamax and 2mM valproic acid. After 7-14 days,
103 secreted recombinant CFD was purified from this media using cobalt immobilised metal
104 affinity chromatography. CFD was eluted in 150mM imidazole in PBS and buffer exchanged

105 by centrifugal concentration (Vivaspin® 20; 10,000Da pore size; Sartorius). Purity of the
106 sample was confirmed on SDS-PAGE and mass spectrometry.

107

108 **Measuring *in vitro* catalytic activity of recombinant FD**

109 Purified human C3b and FB were purchased from Complement Technology, Inc.
110 Recombinant WT, R176P or R176A FD were mixed in varying concentrations (1.0 μ M, 0.2
111 μ M, 0.04 μ M) with C3b (1.0 μ M) and FB (1.0 μ M) in veronal buffer (Lonza) with 10 mM
112 $MgCl_2$ to a final volume of 20 μ L. Reaction tubes were incubated for 10 minutes at 37°C
113 before the addition of sample loading buffer (NuPAGE® LDS Sample Buffer) to terminate
114 the reaction. The samples were then heated to 70°C for 10 minutes and resolved by SDS-
115 PAGE on a Novex NuPAGE 4-12% Bis-Tris Gel. The gels were developed overnight with
116 AcquaStain (Bulldog Bio), washed for 1 hour with distilled water, dried and digitally scanned
117 at high-resolution. Analysis of percentage cleavage of FB was calculated by densitometry
118 analysis using ImageJ 1.x computer software. Statistical comparisons between WT and
119 R176P FD activity were performed at each concentration, from 4 independent experiments
120 using the Kruskal-Wallis non-parametric t-test.

121

122 **Circular dichroism spectroscopy and thermal shift assay**

123 WT and R176P catalytically inactive (S183A) proteins were purified by size exclusion
124 chromatography in chloride-free 0.1M sodium phosphate pH 7.0, diluted to a concentration
125 of 2 mg/mL (72.4 μ M), and loaded into a 0.1 mm quartz sample cell. Circular dichroism
126 spectra were recorded at 20°C on a Jasco J-810 spectropolarimeter equipped with a Jasco
127 PTC-348WI temperature controller. Spectra were acquired from 190-260 nm with 0.1 nm
128 resolution and 1 nm bandwidth. Final spectra are the sum of 20 scans acquired at 50
129 nm/minute. **Thermal shift assay.** 2 μ g of protein was mixed with SYPRO Orange in PBS

130 with 25mM HEPES and fluorescence data acquired on a ViiA 7 real-time PCR system with
131 thermal denaturation over increasing temperatures observed using 1°C intervals.

132

133 **Molecular dynamics (MD) simulation of mutant FD**

134 Starting models were derived from crystal structures of S183A FD (PDB ID 2XW9, 1.2 Å
135 resolution) reported previously.^{E3} The catalytic residue was reverted to serine during the MD
136 setup. Coot^{E4} was used to place the Pro176 side chain in the Arg176 experimental density
137 while minimizing clashes with surrounding atoms and aiming to achieve a favourable initial
138 geometry. The resulting structures were further adjusted in UCSF Chimera.^{E5} The
139 GROMACS package^{E6} was used to set up and run MD simulations. The AMBER99SB-ILDN
140 force field^{E7} and TIP3P water model were used and the structures placed in dodecahedral
141 boxes with 10 Å padding and surrounded with solvent including water and 150 mM NaCl.
142 Following steepest gradient energy minimization, a modified Berendsen thermostat (two
143 groups, time constant 0.1 ps, temperature 310 K) followed by a Berendsen barostat (isotropic,
144 coupling constant 0.5 ps, reference pressure 1 bar) were coupled to the system over 100 ps.
145 100 ns runs of unrestrained MD trajectories were produced. Following removal of periodic
146 boundary condition artefacts, MD runs were visualised and analysed in Chimera and bulk
147 statistics extracted using GROMACS analysis routines.

148

149 **Surface plasmon resonance**

150 Binding experiments were carried out based on established protocol using a Biacore T200
151 instrument.^{E8} FB and FD were buffer exchanged by gel filtration into veronal buffer with
152 10mM MgCl₂. C3b was immobilised on the CM5 chip by amine coupling to achieve 8000
153 resonance units. A dual injection programme was designed where 0.1 μM or 1 μM FB was
154 injected at a flow rate of 30uL/min for 3 minutes, followed by a second injection of a mix of

155 0.1 μM or 1 μM FB and FD at 30 $\mu\text{L}/\text{min}$ for 4 minutes. After 5 minutes for dissociation, the
156 chip was regenerated by three 5-minute washes in 40mM acetate + 3M NaCl (pH 5.5). The
157 chip was re-equilibrated in assay buffer for 5 minutes. Catalytically inactive FD (S183A) or
158 double mutant R176P/S183A were used to emulate the binding response of wild-type or
159 R176P respectively while preventing cleavage of FB and subsequent dissociation of the
160 complex.

161

162 **Esterolytic activity of FD**

163 Z-Lys-SBzl was purchased from Sigma-Aldrich in powder form and reconstituted to 100 mM
164 in 70% DMSO. The assay buffer consisted of 50 mM HEPES (pH7.5), 220mM NaCl and 2
165 mM of Ellman's reagent (5,5-dithio-bis-(2-nitrobenzoic acid) [DTNB]; Sigma-Aldrich). Each
166 reaction mixture contained FD (80nM), variable Z-Lys-SBzl concentrations (0.2-3.2 mM)
167 and 8% v/v of DMSO in a final volume of 200 μl . Solutions were pre-warmed to 37°C before
168 addition of substrate to initiate the reaction. Hydrolysis of Z-lys-SBzl was measured using
169 CLARIOstar FS microplate reader through equimolar formation of chromophore 2-nitro-5-
170 thiobenzoate at 405 nm every 30 seconds for 90 minutes ($\epsilon = 13,600 \text{ M}^{-1}\text{cm}^{-1}$). The rate of
171 hydrolysis was determined from linear slopes of the reaction curves. Reaction velocities,
172 expressed in apparent turnover values were plotted against substrate concentration.

173 **Table E1**

Analyte	Proband	Sibling
Leptin (ng/ml)	10.6	11.3
Adiponectin ($\mu\text{g/ml}$)	9.7	6.5
NEFA ($\mu\text{mol/L}$)	391	212
Cholesterol (mmol/L)	4.2	4
HDL (mmol/L)	1.53	1.26
LDL (mmol/L)	2.3	2.3
Triglycerides (mmol/L)	0.8	0.9
HbA1c (mmol/mol)	36	35

174

175 *NEFA*, non-esterified fatty acids. *HDL*, high-density lipoprotein. *LDL*, low-density

176 lipoprotein.

177 **References**

- 178 E1. Lo JC, Ljubicic S, Leibiger B, Kern M, Leibiger IB, Moede T, et al. Adipsin is an
179 adipokine that improves beta cell function in diabetes. *Cell* 2014; 158:41-53.
- 180 E2. Sprong T, Roos D, Weemaes C, Neeleman C, Geesing CL, Mollnes TE, et al.
181 Deficient alternative complement pathway activation due to factor D deficiency by 2
182 novel mutations in the complement factor D gene in a family with meningococcal
183 infections. *Blood* 2006; 107:4865-70.
- 184 E3. Forneris F, Ricklin D, Wu J, Tzekou A, Wallace RS, Lambris JD, et al. Structures of
185 C3b in complex with factors B and D give insight into complement convertase
186 formation. *Science* 2010; 330:1816-20.
- 187 E4. Emsley P, Lohkamp B, Scott WG, Cowtan K. Features and development of Coot.
188 *Acta Crystallogr D Biol Crystallogr* 2010; 66:486-501.
- 189 E5. Pettersen EF, Goddard TD, Huang CC, Couch GS, Greenblatt DM, Meng EC, et al.
190 UCSF Chimera--a visualization system for exploratory research and analysis. *J*
191 *Comput Chem* 2004; 25:1605-12.
- 192 E6. Abraham MJ, Murtola T, Schulz R, Pall S, Smith JC, Hess B, et al. GROMACS: High
193 performance molecular simulations through multi-level parallelism from laptops to
194 supercomputers. *SoftwareX* 2015; 1-2:19-25.
- 195 E7. Lindorff-Larsen K, Piana S, Palmo K, Maragakis P, Klepeis JL, Dror RO, et al.
196 Improved side-chain torsion potentials for the Amber ff99SB protein force field.
197 *Proteins* 2010; 78:1950-8.
- 198 E8. Katschke KJ, Jr., Wu P, Ganesan R, Kelley RF, Mathieu MA, Hass PE, et al.
199 Inhibiting alternative pathway complement activation by targeting the factor D
200 exosite. *J Biol Chem* 2012; 287:12886-92.

- 201 E9. Lek M, Karczewski KJ, Minikel EV, Samocha KE, Banks E, Fennell T, et al.
202 Analysis of protein-coding genetic variation in 60,706 humans. *Nature* 2016;
203 536:285-91.
- 204 E10. Fredrikson GN, Westberg J, Kuijper EJ, Tijssen CC, Sjöholm AG, Uhlen M, et al.
205 Molecular characterization of properdin deficiency type III: dysfunction produced by
206 a single point mutation in exon 9 of the structural gene causing a tyrosine to aspartic
207 acid interchange. *J Immunol* 1996; 157:3666-71.
- 208

209 **Figure legends**210 **Figure E1:** Mutation R176P results in a type III FD deficiency.211 (A) Chromatograms for the DNA sequence adjacent to position c.602 are shown for each
212 member of the pedigree. The identified variant is rare: the EXAC database reports mutation
213 R176P (variant 19:861943 G/C) at an allele frequency of 1.049×10^{-4} , with no homozygotes.^{E9}

214 (B) Western blot analysis of FD in serum from the patient and healthy control.

215 (C) Secondary structural compositions of WT and R176P FD were evaluated using circular
216 dichroism spectroscopy.217 (D) Comparison of *in vitro* catalytic activity of recombinant WT, R176P, R176Q and R176A
218 FD in terms of FB cleavage. (***, $p < .001$; ****, $p < .0001$).219 (E) Recombinant WT and R176P FD were tested for the ability to reconstitute alternative
220 pathway haemolytic activity when added to FD-depleted serum.

221

222 **Figure E2:** Mutation R176P stabilises the self-inhibited state of FD.223 (A) Structure of free FD^{E3} (PDB ID: 2XW9) showing the catalytic triad (Ser183-His41-
224 Asp89) in an inactive conformation stabilised by the self-inhibitory loop 199-202 (red) and
225 an ion bridge between Asp177 and Agr202. The exosite loops are shown in yellow.226 (B) Structure of C3bB-bound FD^{E3} (PDB ID: 2XWB) omitting the C3b and FB components.
227 FD exosite loops retain a conformation similar to that of unbound FD.228 (C) WT, R176P and R176A structures were stable over 100 ns of unrestrained molecular
229 dynamics simulation with explicit solvent. *RMSD*, root mean square deviation.230 (D) Root mean square fluctuation (RMSF) in WT and mutant FD over the second half of the
231 trajectory.

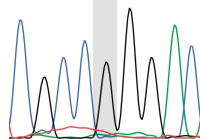
232 (E) Differences in WT versus R176 RMSF mapped to the FD structured. MD predicted
233 increased mobility in exosite loops, notably 155-167, and decreased mobility in loops
234 carrying the catalytic His41 and Asp89 residues.

235

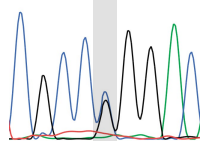
236 **Fig E3:** Assessment of glucose tolerance in patients with functional FD deficiency.
237 Patient and sibling were given 75g of oral glucose at 0 minutes and blood glucose was
238 measured at regular intervals between 0 - 120 minutes. The error bars indicate the range of
239 plasma glucose concentrations between the patient and sibling.

A**Control**

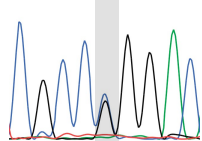
C G C C G G G A C

**I-1**

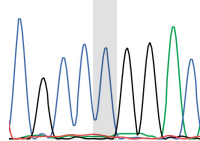
C G C C C G G A C

**I-2**

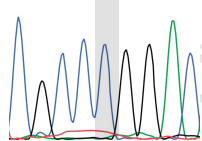
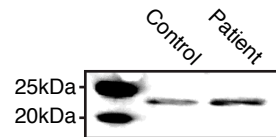
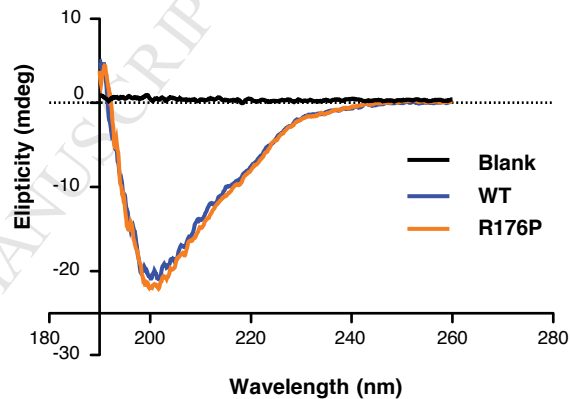
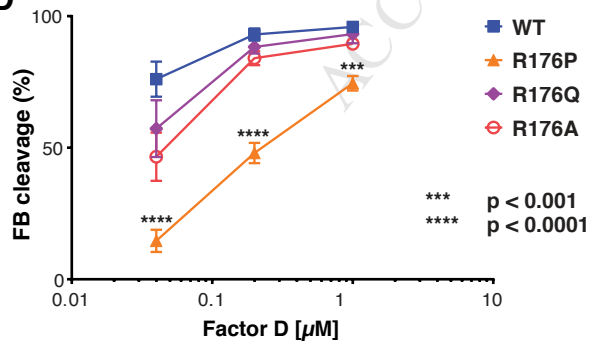
C G C C C G G A C

**II-1**

C G C C C G G A C

**II-2**

C G C C C G G A C

**B****C****D****E**